

2024-01

# Basin scale sources of siltation in a contaminated hydropower reservoir

Bravo-Linares, C

<https://pearl.plymouth.ac.uk/handle/10026.1/21903>

---

10.1016/j.scitotenv.2024.169952

Science of The Total Environment

Elsevier BV

---

*All content in PEARL is protected by copyright law. Author manuscripts are made available in accordance with publisher policies. Please cite only the published version using the details provided on the item record or document. In the absence of an open licence (e.g. Creative Commons), permissions for further reuse of content should be sought from the publisher or author.*

1 Basin scale sources of siltation in a contaminated  
2 hydropower reservoir  
3

4 Claudio Bravo-Linares<sup>a</sup>; Luis Ovando-Fuentealba<sup>a,b</sup>; Enrique Muñoz-Arcos<sup>b</sup>; Jessica  
5 L. Kitch<sup>b</sup>; Geoffrey E. Millward<sup>b</sup>; Ricardo López-Gajardo<sup>a</sup>; Marcela Cañoles-Zambrano<sup>a</sup>;  
6 Alfredo Del Valle<sup>c</sup>; Claire Kelly<sup>b</sup> and William H. Blake<sup>b\*</sup>.

7 <sup>a</sup> Universidad Austral de Chile, Facultad de Ciencias, Instituto de Ciencias Químicas.  
8 Independencia 631, Valdivia, Chile.

9 <sup>b</sup> School of Geography, Earth and Environmental Sciences, University of Plymouth,  
10 PL4 8AA, UK.

11 <sup>c</sup> Foundation for Participatory Innovation, Chile.

12 \* Corresponding author: [william.blake@plymouth.ac.uk](mailto:william.blake@plymouth.ac.uk)

13  
14 Pre-Proof submission: Science of the total Environment

15 Full article available at <https://doi.org/10.1016/j.scitotenv.2024.169952>

16

17 **Abstract**

18 Siltation and the loss of hydropower reservoir capacity is a global challenge with a predicted 26% loss  
19 of storage at the global scale by 2050. Like in many other Latin American contexts, soil erosion  
20 constitutes one of the most significant water pollution problems in Chile with serious siltation  
21 consequences downstream. Identifying the sources and drivers affecting hydropower siltation and  
22 water pollution is a critical need to inform adaptation and mitigation strategies especially in the context  
23 of changing climate regimes e.g. rainfall patterns. We investigated, at basin scale, the main sources of  
24 sediments delivered to one of the largest hydropower reservoirs in South America using a spatio-  
25 temporal geochemical fingerprinting approach. Mining activities contributed equivalent to 9% of total  
26 recent sediment deposited in the hydropower lake with notable concentrations of sediment-associated  
27 pollutants e.g. Cu and Mo in bed sediment between the mine tributary and the reservoir sediment  
28 column. Agricultural sources represented ca. 60% of sediment input wherein livestock production and  
29 agriculture promoted the input of phosphorus to the lake. Evaluation of the lake sediment column  
30 against the tributary network showed that the tributary associated with both dominant anthropogenic  
31 activities (mining and agriculture) contributed substantially more sediment, but sources varied through  
32 time: mining activities have reduced in proportional contribution since dam construction and  
33 proportional inputs from agriculture have increased in recent years, mainly promoted by recent  
34 conversion of steep lands from native vegetation to agriculture. Siltation of major hydropower basins  
35 presents a global challenge exemplified by the Rapel basin. The specific challenges faced here  
36 highlight the urgent need for co-design of evidence-led, context-specific solutions that address the  
37 interplay of drivers both within and without the basin and its communities, enhancing the social  
38 acceptability of sediment management strategies to support the sustainability of clean, hydropower  
39 energy production.

40 **Keywords:** Water-Energy-Food Security, Basin Scale, Sediments, Fingerprinting, Contaminants.

41 **Highlights**

- 42 • Geochemistry allows apportionment of sediment sources impacting hydropower dams
- 43 • Conversion of steep land from native vegetation to agriculture promotes soil erosion
- 44 • Mining is the key source of particulate Cu and Mo in this Andean river basin
- 45 • Sediment-associated Cu, Mo, As and P dominate reservoir contamination
- 46 • This study exemplifies global sediment management challenges in reservoirs

47 CRediT:

48 **Claudio Bravo-Linares:** Conceptualisation; Data curation; Formal analysis; Funding acquisition;  
49 Investigation; Methodology; Project administration; Resources; Software; Supervision; Validation;  
50 Visualization; Writing-original draft; Writing-review & editing. **Ovando-Fuentealba, Luis:** Data curation,  
51 Formal analysis, Methodology, Software. **Muñoz-Arcos, Enrique:** Data curation, Formal analysis,  
52 Methodology, Software. **Kitch, Jessica L:** Data curation, Methodology, Software. **Millward, Geoffrey E.:**  
53 Formal analysis, Writing-review & editing. **López-Gajardo, Ricardo:** Data curation, Formal analysis,  
54 Methodology, Software. **Cañoles, Marcela:** Data curation, Formal analysis, Methodology, Software. **Del**  
55 **Valle, Alfredo:** Writing-review & editing. **Kelly, Claire:** Writing-review & editing. **Blake, H. William:**  
56 Conceptualization; Formal analysis; Funding acquisition; Investigation; Methodology; Project administration;  
57 Resources; Writing-review & editing.

## 58 **1 Introduction**

59 Siltation and the loss of hydropower reservoir capacity is a global challenge and recent analysis  
60 predicts a worldwide storage loss of 26% by 2050 (Perera et al., 2023). While there has been much analysis of  
61 storage capacity and remedial efforts to manage siltation at the reservoir scale e.g. flushing and dredging, there  
62 remain questions about the dynamics of sediment source and delivery at the basin scale to tackle the root cause  
63 of the problem. This study explores how investigation of sediment source dynamics can inform sustainable land  
64 management decisions using the evidence from an exemplar hydropower basin in Chile.

65 Land degradation is a global problem affecting more than 2 billion people (UNCCD and World Bank,  
66 2016). Soil erosion, promoted by multiple factors, has negative impacts on the future of soil fertility, water  
67 quality, food safety and power generation (Dercon et al., 2012; Li and Fang, 2016; Owens, 2020). Future land-  
68 management decisions and water quality assessments in reservoirs require quantification of the anthropogenic  
69 amplification of runoff and soil erosion processes, so that hotspots of soil erosion can be targeted and controlled  
70 by mitigation measures (Collins et al., 2020; Poesen, 2018; Walling, 2013). Erosion processes not only lead to  
71 loss of critical soil resources, but also the associated transport of contaminants that are bound to soil particles,  
72 such as pesticides, heavy metals, radionuclides, and phosphorus, that may have detrimental impacts on the  
73 healthy functioning of water bodies such as rivers, wetlands, lakes and estuarine ecosystems (Rodgers et al.,  
74 2020; Wharton et al., 2017; Wohl, 2015). Fine sediment ( $< 63 \mu\text{m}$ ) has the potential to travel long distances  
75 from source to sink and impact local ecology by reducing water clarity and light penetration (Davies-Colley  
76 and Smith, 2001; Thrush et al., 2004). The identification of sediment sources is therefore essential to implement  
77 focused mitigation actions. Given the widespread impacts of soil erosion and siltation on the food-water-  
78 energy-security nexus (Blake et al., 2021) and the increasingly recognition of multiple co-benefits of natural  
79 capital, basin-wide solutions integrating upstream soil erosion and downstream sediment loading processes are  
80 required to develop sustainable management plans.

81 The impact of agricultural and forestry operations on sediment yields and consequent water pollution  
82 from different catchments, and the effectiveness of potential mitigation measures are traditionally assessed by  
83 measuring the sediment yield from the outlets of small experimental catchments that are subject to different  
84 levels of disturbance/management practices (Stenberg et al., 2015). Whilst this experimental approach can

85 provide an effective basis for assessing the changes in sediment yields, it cannot provide specific information  
86 on the sources of eroded soils, especially when attempting to support collective and integrated decision making  
87 at the basin scale. Such information is essential to design and implement effective sediment control strategies  
88 and to target mitigation measures in the most cost-effective way. The sediment fingerprinting technique has  
89 emerged as a valuable tool in this regard, and it has been applied in a variety of landscapes and settings (Collins  
90 et al., 2020; Owens et al., 2016; Walling, 2013). This technique characterises potential sources according to  
91 their chemical and physical properties. These properties are also measured in sediment samples collected from  
92 areas of accumulation/receiving environments (e.g. dams, rivers, wetlands, lakes, estuaries). Then, potential  
93 sources and mixtures data are analysed, and subsequently mixing models are used to estimate the relative  
94 proportion of soils in a mixture from the various sources in a contemporary and historical perspective (Collins  
95 et al., 2017; Walling, 2013). The tracer properties used must be measurable in both sources and mixtures, be  
96 representative of their sources and must also have conservative signatures from their source, during transport  
97 and deposition (Collins et al., 2017; Owens et al., 2016; Walling, 2013). Several tracer properties have been  
98 used to this purpose: major and trace elements (Blake et al., 2018a; Kitch et al., 2019; Muñoz-Arcos et al.,  
99 2021), Fallout Radionuclides (FRNs) (Schuller et al., 2013), mineral magnetism (Blake et al., 2006; Gaspar et  
100 al., 2019), colour coefficients (Martinez-Carreras et al., 2010) and compound-specific stable isotopes (Blake et  
101 al., 2012; Bravo-Linares et al., 2018). These sediment tracing techniques have been used to determine both  
102 contemporary and historical sources of eroded soils and across a range of spatial scales (Bravo-Linares et al.,  
103 2020; Wynants et al., 2020). However, its application in large river basins, using a tributary tracing approach,  
104 has received little attention to date. This basin scale is critically important when tackling the food-water-energy-  
105 environment challenge, especially in the context of major silted hydropower basin projects in the global South  
106 (Zhang et al., 2018). The present study aims to close this critical gap.

107           Similarly, in many other Latin American contexts, soil erosion constitutes one of the most significant  
108 water pollution problems in Chile. A recent study concluded that 36.8 million hectares of land is subject to  
109 some degree of soil degradation, an equivalent to 49% of the national territory and a further ~7 million hectares  
110 is subject to severe soil erosion. On the other hand, agriculture in Chile has intensified in the past decades  
111 causing changes in the physical properties of soils and consequently creating a potential risk for water erosion  
112 (Fleige et al., 2016). Increased erosion can thus augment sediment loads in waterbodies, especially in

113 hydropower reservoirs, affecting water quality, energy production and inducing reservoir siltation (Bronstert et  
114 al., 2014). In Chile there are 60 dams, which are widely distributed throughout the national territory. This  
115 indeed, has the potential to affect the power generation capacity, as the dams are losing water storage capacity  
116 with increasing sedimentation rates (Kondolf et al., 2014). Particularly in central Chile, the area has eroded  
117 soils (classified into categories of light, moderate, severe and very severe erosion) of 861 thousand hectares,  
118 which represents 52.5% of the regional surface.

119           There is an evident lack of understanding when integrating, in both time and space, impacts of soil  
120 erosion processes from upstream sources to sediment delivery downstream in large scale hydropower systems.  
121 This, of course, brings the need of assessing the sources that are producing siltation in dams and thereby water  
122 pollution through a geographical lens. Here we hypothesised that a tributary tracing fingerprinting approach  
123 can be used to determine the dominant sediment sources for water reservoir siltation and their associated  
124 contaminants at the basin scale as well as the social and environmental drivers. In doing so, we also addressed  
125 the distribution, both spatial and temporal, and potential impacts of sediment associated contaminants in  
126 industrially impacted rivers of similar size across the world.

## 127 **2 Materials and Methods**

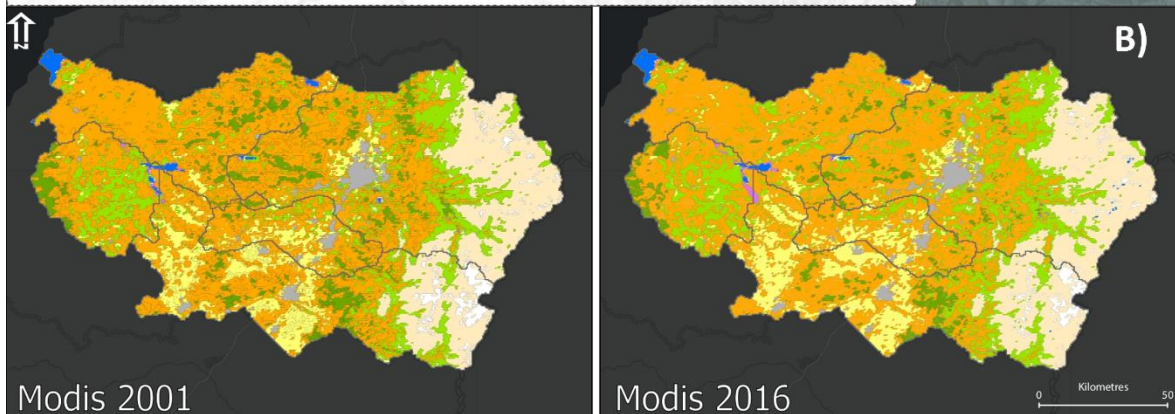
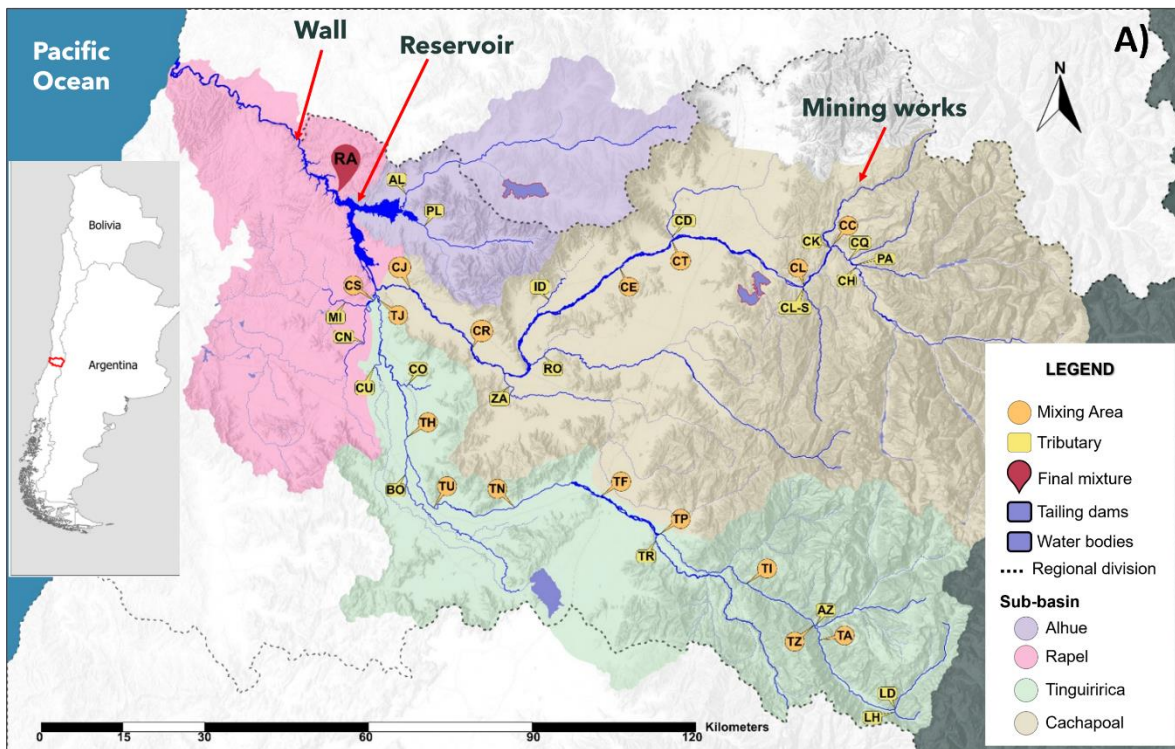
### 128 *2.1 Study Site*

129           This study is based in the Rapel basin, located in Central Chile (VI Region), between the parallels  
130 33°53' and 35°01' south latitude, and with a surface area of 13,695 km<sup>2</sup> (Fig. 1). The annual rain fall by the  
131 coast is 638 mm yr<sup>-1</sup>, 406 mm yr<sup>-1</sup> in the central valley and around 686 mm yr<sup>-1</sup> in the Andes region. Of particular  
132 significance, during the winter of 2023 (July and August) normal rainfall patterns changed dramatically and  
133 two massive flooding events occurred during this period. Here, rainfall concentrated in the Andes produced  
134 dramatic changes in river flow leading to floods that left urban and agricultural areas with substantial amounts  
135 of deposited material. Average temperatures for the coast are 14°C and 9.6°C by the mountains. The catchment  
136 is fed by two main river systems (Cachapoal and Tinguiririca). Cachapoal River is characterised by a nivo-  
137 pluvial regime, with an average flow rate of 172 m<sup>3</sup> s<sup>-1</sup> during winter and 98 m<sup>3</sup> s<sup>-1</sup> during summer, while the  
138 Tinguiririca River has a primarily pluvial regime with average flow rates of 125 m<sup>3</sup> s<sup>-1</sup> during winter and 46 m<sup>3</sup>  
139 s<sup>-1</sup> during summer. Estimated sediment loads, for the Cachapoal and Tinguiririca rivers are approximately 1.11

140 and 0.71 million tons/year, respectively (Pepin et al., 2010). The confluence of these two rivers forms the Rapel  
141 River, which flows into an artificial lake system (Rapel Lake) impounded by a dam (built in 1968) with an  
142 initial water storage capacity of 695 million m<sup>3</sup> and power generation capacity of 350,000 kW.

143           In terms of socio-economic activities, the catchment has been used for hydropower generation since  
144 1968. Upstream, intensive agricultural and forestry activities, mining industry, sand and gravel extraction, land  
145 use changes of hilly zones and recreational uses have severely affected the water storing capacity of the dam  
146 (36% loss by 2010, data provided by national energy company, ENEL). It has been reported that to 2010, 159  
147 million m<sup>3</sup> of coarse material have reached the delta, and another 18 million m<sup>3</sup> of fine sediment have reached  
148 the dam's wall (Lecaros Sánchez, 2011); the latter being the input that provokes greater siltation in the reservoir  
149 and most severe consequences for hydropower generation. These processes have arguably been enhanced by  
150 natural erosion produced by glacial retreat, and the consequences can be seen in the lake environmental quality.  
151 Alongside the sediment load issues, water quality has also been affected by runoff from livestock activities  
152 resulted in a significant input of particulate phosphorous, generating eutrophication and associated issues (Vila  
153 et al., 2000). Moreover, urban development indicated an increase in organic matter and boron (B) (Lacassie and  
154 Ruiz-Del-Solar, 2021).





Rapel Catchment: Changes in land cover 2001 - 2016

Land use	Total area 2001 (ha)	Total area 2016 (ha)	Percentage Change
Water	9360	8613	-7.99
Barren	229993	237282	3.17
Built up area	30694	30919	0.73
Cropland	129014	137377	6.48
Forest	95570	61728	-35.41
Grassland	220362	254011	15.27
Savanna and scrub	684165	675252	-1.3
Snow and ice	26647	19293	-27.6
Wetland	2828	4268	50.95

156 **Fig. 1.A)** Map of the Rapel Basin location in central Chile indicating their sub-basins and sediment sampling  
157 sites given by their acronyms. Cachapoal sub-basin: PA: Pangal river, CQ: Clonqui stream, CC: Cachapoal  
158 river at Clonqui stream confluence, CH: Cachapoal river in the Andes, CK: Coya river, CL-S: Claro river of  
159 Cauquenes, CL: Cachapoal river at Claro river confluence, CD: Cadena stream (in Cachapoal river catchment),  
160 CT: Cachapoal river at Punta Cortés, CE: Cachapoal river at Doñihue, ID: Idahue stream, RO: Claro river of  
161 Rengo, ZA: Zamorano stream, CR: Cachapoal river at La Ratonera and CJ: Cachapoal river at La Junta.  
162 Tinguiririca sub-basin: LH: Lo Herrera stream, LD: Las Damas river, TA: Tinguiririca river in the Andes, AZ:  
163 Azufre river, TZ: Tinguiririca river at Azufre river confluence, TI: Tinguiririca river at La Iglesia, TR: Negro  
164 river, TP: Tinguiririca river at Puente Negro, TF: Tinguiririca river at San Fernando, TN: Tinguiririca river at  
165 Nanchagua, TU: Tinguiririca river at Cunaco, BO: Chimbarongo stream, TH: Tinguiririca river at Huique. CO:  
166 La Condénada stream, CU: Cunaco stream and TJ: River Tinguiririca at La Junta. Rapel sub-catchment: CN:  
167 Las Cadenas stream, MI: San Miguel stream and CS: Las Cadenas stream at the confluence between San Miguel  
168 and Las Cadenas streams. Alhué sub-basin: AL: Alhué river and PL: Las Palmas stream, and RA: Rapel lake.  
169 B) Land use maps and C) Land use changes (%).

170 The Rapel Basin is dominated by a Mediterranean climate (Aitken et al., 2016). The catchment is  
171 characterised by a tectonic topography, which includes the Andes Mountain range to the east and the lower  
172 elevation Coastal Range to the west. The topography and millennial-scale denudation and deposition processes  
173 have resulted in the creation of two lowland plains in between the ranges, with fertile soils that have become  
174 increasingly dominated by intensive agricultural production since the late 20<sup>th</sup> Century. Land cover varies along  
175 the stream profile in the catchment (See Fig. 1). Upstream, barren land with natural vegetation is most common.  
176 Along the coastal range and throughout the lowland plain cropland, evergreen forest and savannah are dominant.  
177 The coastal range is the area where agricultural activity is concentrated. Cultivation of this land has been  
178 increasing within the basin (~7%), as more olive trees, avocado orchards, citrus and vineyards have been planted  
179 on hilly zones in response to market demand and commercial opportunities for expansion. Changing land use  
180 practices is hypothesised to have increased erosion risk, where permanent native flora cover is lost through  
181 clearance and tillage for cultivation. In addition to the long-term trend for extensively managed montane pasture  
182 to be converted into fruit and grain production, cultivation patterns within the lowlands also are subject to  
183 temporal variation (Schulz et al., 2010).

184 Copper (Cu) mining covers a small area within the catchment. It is an important economic activity in  
185 the basin. The state mining company operating here is one of the biggest underground mines in the world and  
186 produced near 460 thousand metric tons during the year 2021. It is located in the Andes and mining products  
187 (Cu) have the potential to enter the river network through the Coya River which feeds into the Cachapoal River  
188 (Pizarro et al., 2003), contributing other metals such as Molybdenum (Mo) and Antimony (Sb) to the  
189 sedimentary signature of this river (Lacassie and Ruiz-Del-Solar, 2021).

190 *2.2 Sampling strategy to evaluate sediment source dynamics: the tributary tracing approach.*

191 The sediment fingerprinting technique can be implemented by using several tracer properties that are  
192 representative of characteristics of the main sources within the catchment (Haddadchi et al., 2013).  
193 Nevertheless, not all properties may account to all different characteristics (e.g. land uses) when basins are  
194 inherently complex. Due to the wide variety of natural and anthropogenic activities carried out in the catchment,  
195 including mining, agriculture (several crops), livestock, industrial, and urbanisation, we used major and minor  
196 element geochemical fingerprints as a comprehensive approach likely to ascribe sediment sources and  
197 subsequent water pollution in this context.

198 The tributary approach for sediment fingerprinting involved sampling in the different upstream  
199 tributaries and using them as potential sediment sources (Lacey et al., 2017). Since most of the significant  
200 particle size effects occur typically during the initial stages of mobilisation and transportation from slope to  
201 channel, leading to potential particle size enrichment or depletion on fingerprinting properties, the tributary  
202 tracing approach offers a means to account for these variations (Lacey et al., 2017). In this study, an  
203 assumption that tributary sediments comprise a composite mixture of eroded sediment from the tributary  
204 catchment dominant sources has been made (Wynants et al., 2020).

205 Approximately 300 sediment samples were collected at different locations in the Rapel lake and its  
206 main tributaries during 2019 (Fig. 1): Alhué, Las Palmas, Cachapoal, Tinguiririca and Las Cadenas. At every  
207 tributary, 7 to 10 spatially integrated channel bed deposited sediment samples were taken upstream of the  
208 confluence where recent sediment deposits were clearly evidenced. With regards to Tinguiririca and Cachapoal  
209 sub-catchments, low order tributaries to their higher order mainstem were also sampled before the confluence  
210 to capture characteristics of lowland feeder streams (Fig. 1). Surficial sediments were sampled using plastic

211 spatulas to avoid cross contamination, placed in double plastic bags and the central point of each sampling area  
212 was recorded using a GPS. Hence, the surficial sediment samples were used in the following context: First:  
213 Recently deposited sediments collected at the main rivers and tributaries were employed to characterise the  
214 signature of dominant sources within the tributary catchment. Second: Sediment samples collected in the lake  
215 (sediment mixing/accumulation zone) were used to estimate the contribution of the different upstream tributary  
216 sediments. Of note, Additional sampling points presented in the map were only considered when evaluating the  
217 contaminant distribution along the river channel and not for sediment source apportionment.

218 Sediment cores (n = 6) were taken in the upper zone of the reservoir during 2020 (around 12 km from  
219 the wall and around 22 km from the confluence of the two main tributaries). The sampling was done in a  
220 meander area that was selected as a natural and representative sediment accumulation zone (Fig.1. Lat. -  
221 34.113278°; Long. -71.516222°). The average water depth was 30 m. This location represented the maximum  
222 feasible depth for coring with depths at the centre of the dam and places near to the wall reaching greater than  
223 50 m. The samples were collected from an anchored zodiac using a Ubitech gravity core equipped with acrylic  
224 tubes of 2.5 m length and 6 cm of internal diameter. Sediment core depths ranged from 88 to 122 cm. In parallel,  
225 surficial sediment samples (3 samples with 3 to 5 sub-samples for analysis) were taken using a Van Veen grab  
226 sampler and short-cores (about 10 – 15 cm of sediment depth) to assess contemporary sediment source  
227 contributions and spatial variability therein.

### 228 2.3 *Sample preparation and analysis*

229 Riverine sediments were oven-dried at 60°C for 3 to 4 days, sieved through a 2 mm sieve and then  
230 through a < 63 µm mesh with the fine fraction packed into plastic bags for further analysis. Core samples were  
231 sliced every 2 cm immediately after sampling, placed in double Ziploc plastic bags and subsequently dried  
232 using a drying cabinet at 60°C. Samples were gently disaggregated with a pestle and mortar, then packed for  
233 further analysis.

234 A subsample of approximately 1 g of dried and sieved particles was used for particle size analysis  
235 using a Malvern 2000 series laser granulometer. Herein, 3 ml of 6% Hydrogen Peroxide (H<sub>2</sub>O<sub>2</sub>) was added to  
236 every sample to remove organic matter over a 12-hour period. Subsequently, another aliquot of 6% of H<sub>2</sub>O<sub>2</sub>  
237 was added to each sample to assess if effervescence still took place. Samples were then placed into a water bath

238 at 80°C for 2 to 4 hours and cooled at room temperature. Before laser diffraction analysis, sodium  
239 hexametaphosphate was added to every sample as a dispersant. Particle size distribution analyses were  
240 performed in triplicate and results were assessed statistically to check for large dispersion between particle size  
241 distributions percentiles in which a coefficient of variation < 10 % between percentiles was accepted as a valid  
242 result.

243 Samples were analysed for major and minor elements by Wavelength Dispersive X-Ray Fluorescence  
244 (WD-XRF, PANalytical Axios Max) as pressed pellets. The sieved < 63 µm fraction was homogenised by  
245 milling for 20 min at 300 RPM, mixed with Ceridust 6050M S1000 polypropylene wax binder, packed into  
246 aluminium cups and pressed into pellets. The instrument was operated at 4 kW using a Rh target X-ray tube.  
247 During sequential elemental analysis, tube settings ranged from 25 kV, 160 mA for low atomic weight elements,  
248 up to 60 kV, 66 mA for higher atomic weight elements. All analyses were carried out using the “Pro Trace”  
249 analysis application. For Quality Control, analyses of random samples were carried out in triplicate to evaluate  
250 method precision. Results showed a relative standard deviation ranging between 0.5 to 31% for all elements  
251 analysed. Instrument performance is validated by routine analysis of certified stream sediment reference  
252 material (NCS DC 73309) where recovery is typically within ±10% from certified values. Instrumental Limits  
253 of Detection (LoD) were obtained, and instrumental drift (using a multielement glass sample) were also checked  
254 during sample runs.

255 From the six cores taken, the deepest (122 cm) was selected to perform sediment geochronology and  
256 thereby estimating sedimentation rates via fallout <sup>210</sup>Pb (Appleby, 2001). This deepest core was selected for  
257 profiling to minimise the risk of disturbance due to seasonal emptying and filling of the lake for  
258 recreational/hydropower generation purposes. <sup>210</sup>Pb, <sup>214</sup>Pb, <sup>137</sup>Cs and <sup>241</sup>Am activity concentrations were  
259 measured using a well type HPGe gamma spectrometer. Total <sup>210</sup>Pb was determined via its gamma emissions  
260 at 46.5 keV, <sup>226</sup>Ra (to determine the supported <sup>210</sup>Pb component) by the 295 keV and 352 keV gamma rays  
261 emitted by its daughter isotope <sup>214</sup>Pb, and <sup>137</sup>Cs was measured by its emissions at 662 keV (Appleby, 2001).  
262 The CRS (Constant Rate of Supply) model (Appleby and Oldfield, 1978) was applied to construct core  
263 chronologies and sedimentation rates from activity concentrations. Since the reservoir was constructed after the  
264 <sup>137</sup>Cs peak fallout in the 1960s, there was a lack of an independent chronological marker. The CRS-model dates

265 were benchmarked to the basal core base date by reservoir construction in 1968 and the subsequent  
266 chronological estimate was independently evaluated by comparing sedimentation rates patterns through time to  
267 floods records from the main tributaries in the upper part of the core (Fig. S1). All samples were analysed at  
268 the ISO9001 certified University of Plymouth Consolidated Radioisotope Facility (CoRIF), UK.

## 269 2.4 *Statistical analysis and mixing modelling*

### 270 2.4.1 *Tracer selection*

271 An important aspect before performing any calculation for geochemistry-based sediment  
272 apportionment is the determination of relevant tracers. From 44 elements analysed, tracers to be used in the  
273 mixing model were selected as follows: (a) Firstly, we removed all the elements that were below the  
274 instrumental limit of detection (see Table S1); (b) we removed the elements that have the potential to be soluble  
275 and may present issues of transformation of the signatures from the released sediment to the final sink. This  
276 criterion was done according to the 90% ratio between natural dissolved and total elemental river transport  
277 (Collins et al., 2020). The elements discarded were Cl, Br, S, Na, Sr, Ca, Sb, Mg, Mo, As, Ba and K. (c) a  
278 further selection procedure based on boxplots was applied (Ovando et al., accepted for publication). In brief,  
279 those tracers that fulfilled the following criteria were selected: 1) The median of the mixture lies inside the  
280 maximum third quartile and minimum first quartile among the sources. 2) The mixture distribution lies within  
281 the maximum and minimum median among the sources. 3) Considering just the sources, there was a positive  
282 difference between the maximum first quartile and minimum third quartile. 4) At least, one of the sources  
283 distributions has to be different from the mixture distribution. Finally, d) source and mixture particle size  
284 distributions were assessed and relationships with element concentrations were evaluated through correlation  
285 analysis where required (Lacey et al., 2017). After the tracer selection procedure, Principal Component  
286 Analysis (PCA) was conducted to visualise source and mixture groupings in the ordination plot along the first  
287 two main principal components retained based on their percentage of explained variance. Tracer selection and  
288 PCA were performed using R statistical package.

### 289 2.4.2 *Mixing model structure*

290 The mixing model employed was MixSIAR (Stock et al., 2018). The model was run with  
291 uninformative prior, error structure as 'residual error' and chain length of 'very long'. Convergence of the model

292 was evaluated using the Gelman-Rubin diagnostic, in which case all variables were below 1.05. This in accord  
293 with accepted limits in this field of application (Blake et al., 2018a; Smith et al., 2018). All results are provided  
294 as the mean and standard deviations as well as credible intervals from the posterior distributions.

### 295 **3 Results and discussion**

#### 296 *3.1 Tracer selection*

297 The potential influence of particle sorting effects on sediment fingerprinting properties (e.g. element  
298 concentrations) have been widely debated in the literature (Gaspar et al., 2022; Lacey et al., 2017; Smith and  
299 Blake, 2014). Differences in grain size between soil and sediment particles can bias mixing model results  
300 (Gaspar et al., 2022). To address the potential effects, several approaches have been applied such as sample  
301 fractionation and particle size correction factors. However, it has been reported that the use of particle size  
302 correction factors can lead to overcorrection (Smith and Blake, 2014). Here, a similar approach to that reported  
303 in Smith et al., (2018) and Gaspar et al., (2022) where evaluation of potential grain size effects was carried out.  
304 Differences in the median particle size distribution (D50) between tributary and lake sediments were found (see  
305 Fig. S2). Therefore, a correlation analysis between the Specific Surface Area (SSA) and elemental  
306 concentrations of all tributary samples was performed (Table S2). Only one element (out of 27) showed strong  
307 correlation with SSA (i.e. Cr,  $R = -0.55$ , see Table S2) while four presented moderate association (i.e. V, Mn,  
308 Rb and Cs.  $R$  between  $-0.3$  and  $-0.5$  or  $0.3$  and  $0.5$ , see Table S2) and six elements had weak although significant  
309 correlations (i.e. Fe, Ni, Zn, Zr, Pb and U.  $R$  between  $-0.2$  and  $-0.3$  or  $0.2$  and  $0.3$ ,  $p < 0.05$ ,  $n = 60$ ).  
310 Consequently, due to low association between these elements and SSA, instead of removing them (or going  
311 further in particle size effects assessment) we tested them within the tracer selection procedure (see section  
312 2.4.1). Here, the inclusion of some weak-to-moderate correlated tracers was not considered likely to increase,  
313 or significantly influence the source apportionment results.

314 It is noteworthy that when performing historical sediment source apportionment, it may not be  
315 appropriate to use elements coming from pollution point-sources (such as Cu from mining in this study) due to  
316 changes in concentrations along the core profile in relation to pollutant dynamics compared to contemporary  
317 source samples used to characterise the input. This implies that those elements may be discarded during the  
318 tracer selection procedure for some mixtures and included in others. For instance, range test evaluation of Cu

319 concentrations at the top of the core suggest inclusion of this tracer in the modelling, while the opposite occurs  
 320 when evaluating the fit of sediment from the bottom (Fig. S3). The influence on the inclusion of Cu in the tracer  
 321 set for modelling can be seen in sections 6 and 7 of the core, where results did not differ significantly when Cu  
 322 is included (section 7) and not included (section 6) (see Table S5), possibly due to the number of tracers  
 323 employed in a single calculation (between 12 to 18). Here, it is expected that one rogue tracer would not  
 324 significantly drive or influence mixing model outputs.

325 The effect of tracer selection procedure was assessed using principal component analyses. It was found  
 326 that for each mixing area (Fig. S4a – e): 1) mixture data points always fell within the source factor space, 2) in  
 327 general, source (tributary) groupings presented low dispersion, and 3) discrimination among source groups  
 328 improved. The explained variance ranged from 56.8 to 81.8% which can be considered acceptable for all PCAs  
 329 performed.

### 330 3.2 Sediment source apportionment

#### 331 3.2.1 Contemporary source apportionment

332 To visualise the sediment apportionment at different scales within the catchment, calculations were  
 333 performed at different mixing areas in the two main rivers (Cachapoal and Tinguiririca) and the final mixture  
 334 (Rapel Lake). The results obtained are detailed in Table 1.

335 **Table 1.** Spatial contemporary source apportionment summary statistics obtained from MixSIAR for  
 336 the Rapel catchment (SD: Standard Deviation and CI: 95 % Credible Interval).

	Mixing Zone	Sources	Mean contribution (%)	SD	CI
Cachapoal	CL	CH	2.7	1.8	0.1 - 6.9
		CK	81.4	4.7	71.7 - 90.1
		CQ	1.7	1.7	0.04 - 5.9
		PA	14.2	5.0	4.6 - 24.1
	CR	CD	3.5	3.2	0.1 - 11.9
		CL	17.3	4.0	8.9 - 24.9
		CL-S	9.3	4.0	1.7 - 17.5
Tinguiririca	TF	ID	5.7	5.0	0.2 - 18.9
		RO	60.5	8.9	40.1 - 76.0
		ZA	3.7	3.2	0.1 - 12
Tinguiririca	TF	AZ	32.8	6.3	19.6 - 44.5
		LD	7.1	5.6	0.2 - 20.9
		LH	14.9	6.2	3.3 - 27.4



		TR	45.2	7.7	30.0 - 60.3
		BO	6.3	3.9	0.5 - 15.1
	TJ	CO	5.7	3.4	0.5 - 13.6
		CU	37.3	8.2	20.3 - 53.0
		TF	50.7	7.1	37.2 - 65.2
		AL	12.5	7.8	0.9 - 29.6
		CR	63.2	10.6	39.3 - 81.6
Final Mixture	RA	CS	5.5	4.4	0.2 - 16.0
		PL	11.1	7.6	0.5 - 28.5
		TJ	7.8	7.0	0.2 - 25.9

337

338 The Cachapoal river sub-catchment was divided in two calculation sections (Table 1). The upstream  
339 portion draining the Andes Mountains was evaluated in the first mixture area in the Cachapoal confluence with  
340 Claro River (CL sampling site). Details of tracers selected, discarded, etc. can be seen in Table S4. Results at  
341 this point indicated that the dominant source at the CL mixing point was the Coya River (CK) with  $81.4 \pm 4.7$   
342 %, followed by the Pangal River (PA), Cachapoal Andes (CH) and Clonqui River (CQ) with contributions of  
343  $14.2 \pm 5.0$ ,  $2.7 \pm 1.8$ ,  $1.7 \pm 1.7$  % respectively. These results were in agreement with tributary groupings  
344 observed in Fig. S4.a, where CK samples clustered together with CL-M samples. The main sediment source to  
345 this point comes from the tributary that has a strong signal of mining activities with significant influence of Cu  
346 (see PCA Fig. S4.a). The next mixing area was the Cachapoal at the “La Ratonera” sampling point (CR). A  
347 further point and closest to the confluence of the two main rivers was the Cachapoal at “La Junta” (CJ).  
348 However, due to the river being canalised for irrigation, a large proportion of fine sediment bearing flow is  
349 diverted into the agricultural area. Subsequently, little water reaches the CJ point. For this reason, the CR  
350 sampling point was used to represent the integrated sediment input from upstream (with no river intervention).  
351 The results from the mixing model to this point showed that the main sources (tributaries) were the Claro River  
352 (RO) with  $60.5 \pm 8.9\%$ , followed by CL with  $17.3 \pm 4$  % and Claro River of Cauquenes (CL-S) with  $9.3 \pm 4.0\%$ ,  
353 the rest were distributed between 3.5 to 5.7 % of contribution (CD, ID and ZA). The dominant contribution of  
354 RO sediments to CR mixing point is expected as RO is a river that carries sediments from agricultural areas  
355 along the whole central valley and delivers them close to the mixing point (~ 10 km). Similarities in geochemical  
356 sediment signatures can be confirmed by looking at the PCA score plot where RO samples are overlapping the  
357 CR sample cluster (Fig. S4.b). It is important to emphasise that we considered the previous mixing point CL as  
358 a source for the second mixing area evaluated and not the individual tributaries from the first mixing area. Also,

359 the contribution of CL to this point is expected to be highly influenced by the sediments coming from the Coya  
360 River (CK) whose contribution was more than 80% to mixing point CL. Nevertheless, when performing the  
361 full calculation of all tributaries upstream of CR, the main contributions did not change considerably (e.g. RO  
362 from 60.5 to 62.5% data not shown). It is not surprising that the tributary RO is the main source as it flows  
363 through the whole Central Valley carrying sediments from the agricultural activities and delivering its sediments  
364 very close to the mixing point CR (~16 km).

365         Considering that a tributary transports sediment that integrates the inputs from its catchment area  
366 (Haddadchi et al., 2013), we renamed and summed the individual contributions of each tributary to the final  
367 point of the river according to the main land uses/activities occurring in the Cachapoal sub-catchment. Results  
368 showed that the 73% of the sediment contributions originated from areas that harboured agricultural activities  
369 in the Central Valley. The other comes from the mining activity conducted in the Andes with 14%, and finally  
370 that which is derived from the Andes attributed to natural erosion processes such as snow melting and glacial  
371 retreat inputs contributing 13%.

372         Regarding the Tinguiririca sub-catchment, at the first mixing zone (sampling point TF, Table 1) the  
373 main sediment source was derived from the Claro River at Puente Negro (TR) ( $45.2 \pm 7.7\%$ ), followed by  
374 Azufre River (AZ) with  $32.8 \pm 6.3\%$  and finally Tinguiririca Andes at Lo Herrera stream (LH) and Las Damas  
375 River (LD) with  $14.9 \pm 6.2$  and  $7.1 \pm 5.6\%$  respectively. At the second mixing point, La Junta (TJ), results  
376 indicated that the main contributor were the previous mixing point area TF with  $50.7 \pm 7.1\%$ , then tributaries  
377 Calleuque stream (CU) ( $37.3 \pm 8.2\%$ ), and the others (CO, BO) contributed the remaining 12%. Considering  
378 the same assumption applied to the Cachapoal sub-catchment, the integration of results from these 'type'  
379 tributaries suggested that the dominant sources that contributed to this mixing point in the Tinguiririca river  
380 were derived from the Andes tributaries (51%) followed by tributaries that drain agricultural activities in the  
381 Coastal Range area (43%) and tributaries that hold agriculture activities in the Central Valley (6%)

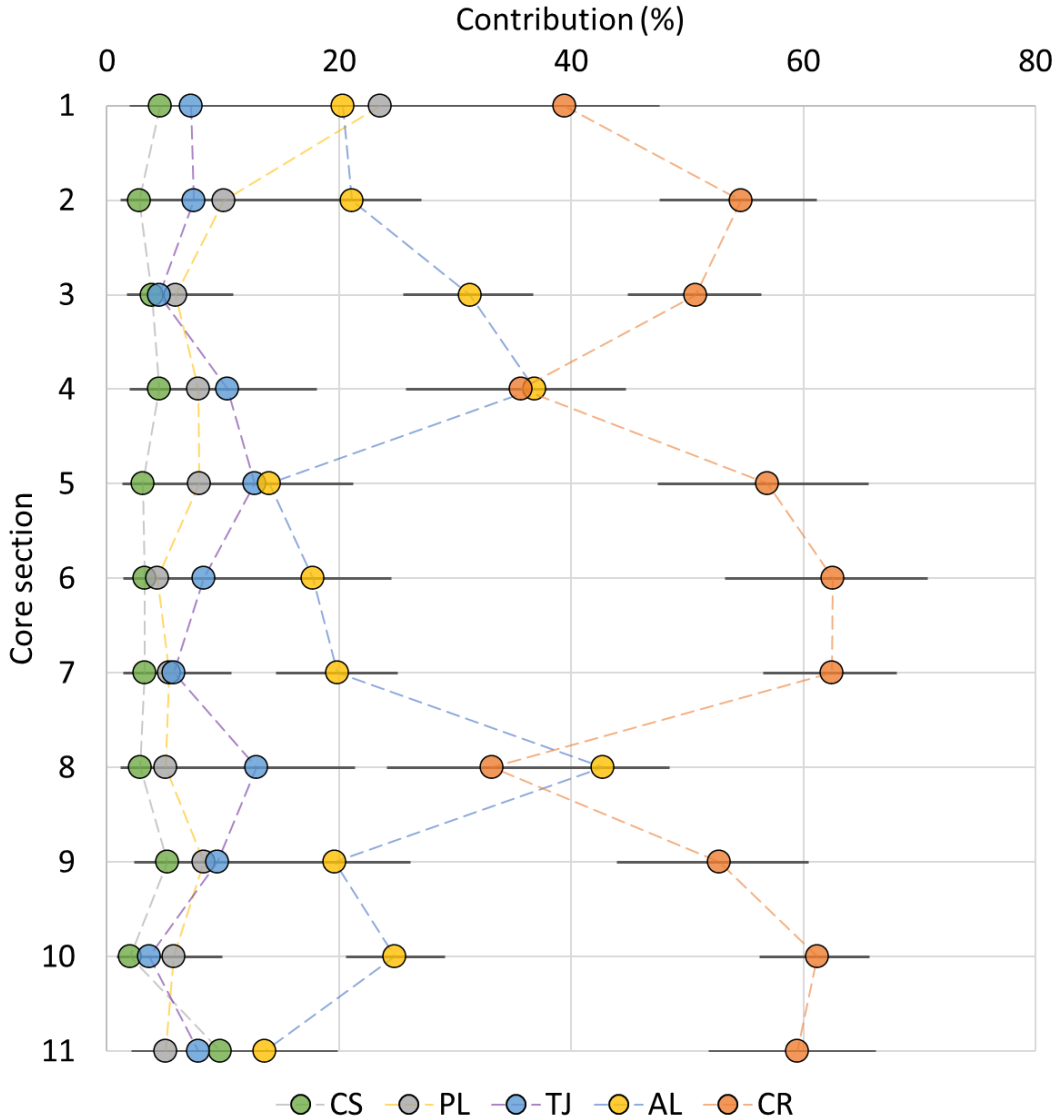
382         For the final mixture zone at the Rapel lake (Fig. 1), the source points were selected from the lowermost  
383 sampling point of each sub-basin as a representative composite of the sediments derived from each. These  
384 included the sampling points at the two main rivers (CR: Cachapoal river and TJ: Tinguiririca river) as well as  
385 the independent sources that contribute directly to the Lake (AL: Alhue river, and PL: Las Palmas stream-in

386 Las Cabras sub-catchment and CS: Las Cadenas stream). Differences in tributaries sediment geochemical  
387 composition were clearly observable after the tracer selection procedure (see PCA score plot in Fig. S4.e) which  
388 indicates that anthropogenic activities exert a significant influence on the riverine sediment geochemical  
389 signatures even in catchments under similar geology (e.g. Alhué and Las Cabras catchments). Apportionment  
390 results indicated that the Cachapoal sub-catchment (CR) was the main source to the final mixing area with a  
391  $63.2 \pm 10.6\%$ , followed by Alhue sub-catchment (AL) with  $12.5 \pm 7.8\%$ , Las Cabras sub-catchment (PL) with  
392  $11.1 \pm 7.6\%$ , Tinguiririca sub-catchment (TJ)  $7.8 \pm 7.0\%$  and finally Las Cadenas sub-catchment (CS) with  $5.5$   
393  $\pm 4.4\%$ .

### 394 3.2.2 *Temporal variability in sediment source contributions to the lake*

395 The activity concentration depth profile of fallout  $^{210}\text{Pb}$  (Fig. S5) showed a profile typical of a dynamic  
396 sedimentation rate with a lack of an exponential profile, rather it had notable peaks and troughs linked to  
397 depositional episodes. The lack of an independent fallout radionuclide marker (e.g.  $^{137}\text{Cs}$ ) led to a key  
398 assumption that the deepest part of the core was the date when the dam was built (1968-69). Additional evidence  
399 of major flow events from river flow gauge records was then utilised to corroborate the resultant geochronology.  
400 This information was derived from four permanent stations within the two main rivers that have records  
401 extending back to 2003. Assuming that some physical phenomena that occurs in the upper and lower part of the  
402 catchment will affect the water/sediment load of the lake, we plotted some parameters such as stream flow ( $\text{m}^3$   
403  $\text{s}^{-1}$ ) and sediment concentration ( $\text{mg L}^{-1}$ ) alongside the mass accumulation rate (MAR) estimated from the  
404 geochronology model (Fig. S1). From these plots, the moving average of the stream flow showed a close  
405 relationship with MAR for the dated core (Fig. S1). This coherence in records provided support for the relative  
406 derived dates allowing us to proceed in using changes in sedimentation rates to structure sediment data for  
407 unmixing purposes. Consequently, the number of core sections considered were 11.

408 Historical source apportionment of each section showed that the historical dominant sediment source  
409 has been the Cachapoal river (CR) contributing from 33-63%, followed by the Alhue river-AL (14-43%) and  
410 finally the other three tributaries (CS, PL, and TJ) with minor contributions ranging from 2-24% (See Fig. 2  
411 and Table S3 for summary statistics).



412

413 **Fig. 2.** Historical tributary source contribution (%) for each core section obtained from MixSIAR mixing  
 414 model. Points indicates median relative contribution and error bars 50% credible intervals. Core sections  
 415 indicate cumulative depth from bottom: 108-120cm (11) to top 0-6cm (1) with deposition period from 1968-  
 416 1976 (11) to 2017-2019 (1). CS: Las Cadenas stream, PL: Las Palmas stream, TJ: Tinguririca river at La Junta,  
 417 AL: Alhué river and CR: Cachapoal river at La Ratонера.

418 Tributaries were classified according to the main activities performed in their catchment area (Andes-  
 419 Natural erosion, Mining and agricultural activities, as in section 3.2.1). Here, the historical contributions (see  
 420 Fig. S6) are much clearer and in agreement with catchment antecedents, as historical contributions from the

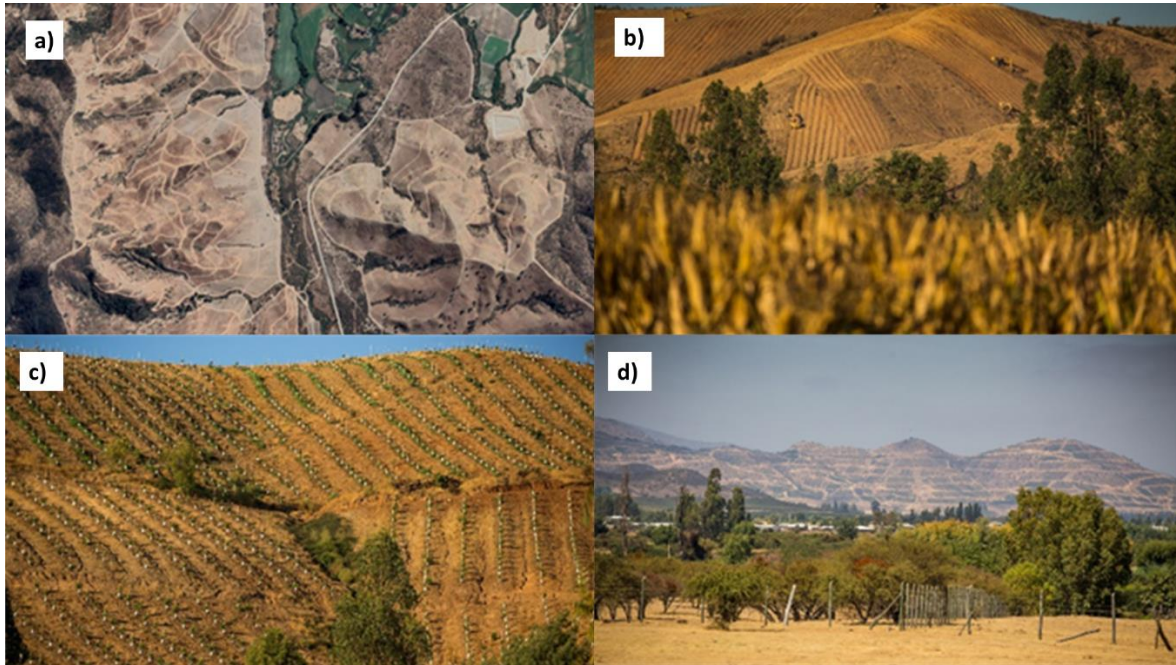
421 Andes have been relatively constant, mining has decreased, and agricultural inputs have increased throughout  
422 the years.

### 423 3.2.3 *Causes of siltation in the Rapel lake.*

424 There are various causes of siltation in the Rapel Lake. On the one hand, field observations suggest  
425 that both main rivers (i.e. Cachapoal and Tinguiririca rivers) carry substantial amount of sediment from the  
426 Andes mountains (especially in summer), with significant contributions from tributaries along the central valley  
427 and the coastal range where changes in sediment colour and turbidity are clearly observable. Of the two main  
428 rivers, the Cachapoal river contributed the majority of sediment (~63%), at least 8 times higher than the  
429 Tinguiririca river (~8%) in a contemporary context. This is in agreement with overall flow regimes of each river  
430 (see river flows information on section 2.1 and Fig. S1). Nevertheless, natural sediment sources represented by  
431 glacier retreat and snow melting from the Andes, in light of the current findings, were low. On the other hand,  
432 the Alhué river (AL) contribution is associated to agricultural activities and, to a lesser extent, copper mining  
433 refining activities. Even though, it is much closer to the mixing area selected it is not expected to contribute  
434 sediments significantly due to low river flow compared to Cachapoal and Tinguiririca rivers (Alhué stream  
435 contributes around 12% of the total flow into the lake and it has an mean annual flow of  $2.0 \text{ m}^3 \text{ s}^{-1}$  (Rossel and  
436 de la Fuente, 2015)). However, its contribution resulted higher than the Tinguiririca river.

437 Agricultural activities across the system are also an important source of fine sediment to the lake. For  
438 instance, around 60% of CR mixing point contribution comes mainly from agriculture (RO tributary, see section  
439 3.2.1) and the historical contribution of PL stream (dominated by agricultural activities) presented an increment  
440 in the top two sections of the core (Fig. 2). This contribution goes against local expectation of low input from  
441 agricultural land which historically occupies the low gradient/flat terrain of the basin floor. Recent years,  
442 however, have seen important land use changes, where steeper terrain of the Coastal Range has been cleared of  
443 natural vegetation and planted with vineyards and avocado, olive and citrus trees (Fig. 3a, c and d). These land  
444 use changes can be seen on Fig. 1b and c. where croplands have increased by ~7% and forest have decreased  
445 ~35%. These changes have been observed predominantly on hilly areas by the Coastal Range (Fig. 3b, c and  
446 d). This conversion of steeper terrain from natural vegetation to agriculture, in response to economic drivers to  
447 increase production, have generated an important sediment load transferred into the lake. Clearance of the

448 secondary forest of hilly zones and conversion to agricultural use relies on heavy machinery leading to  
449 compaction wherein plough lines are required to be parallel to the slope due to the steep gradient and safe  
450 operation of machinery (Fig. 3b). Overall, conversion of land from natural to agricultural usage generates areas  
451 of bare soil with compacted tracks aligned with the steep slopes leaving a landscape highly prone to erosion.



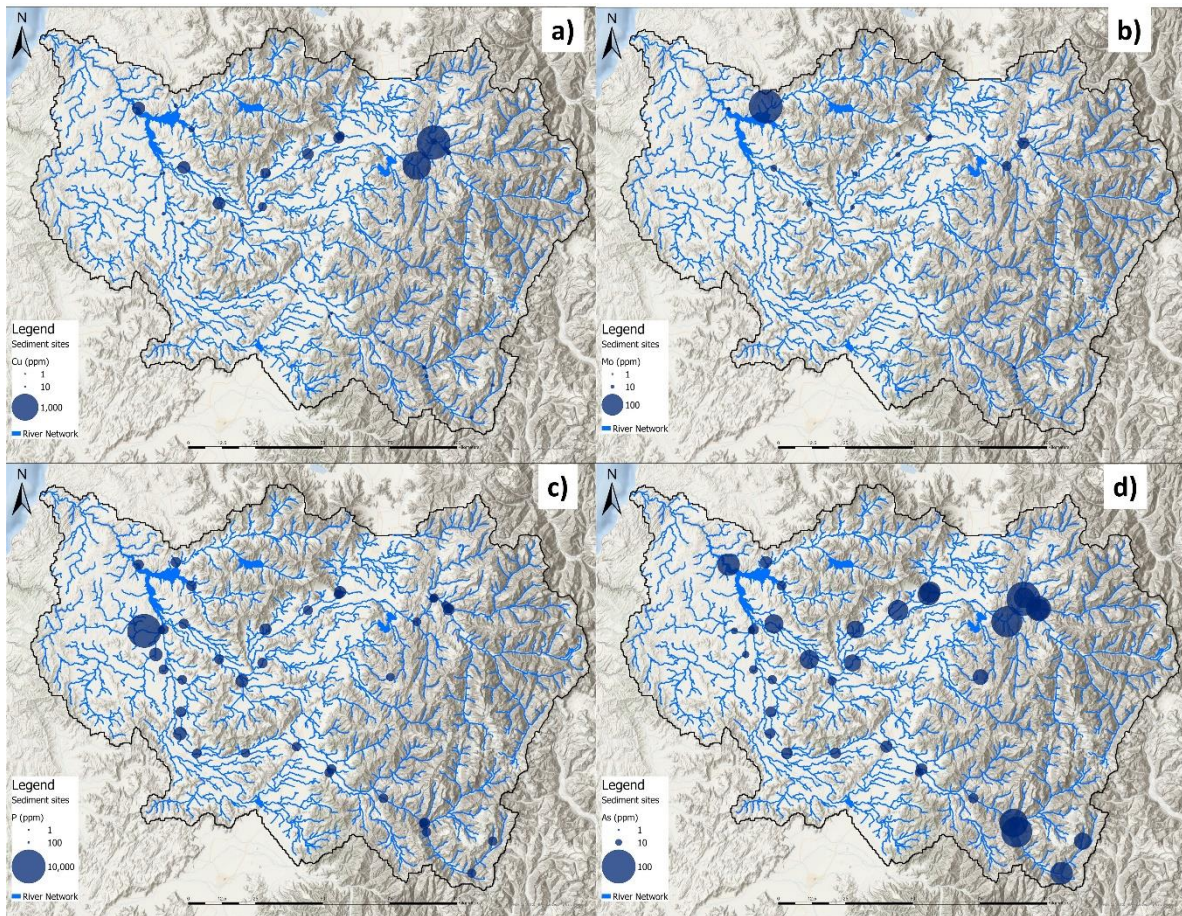
452

453 **Fig. 3.** Images of the land use changes in the Coastal Range area. a) Satellite Google Earth image  
454 showing hillslope clearances; b) Land reconversion for cropping; c) and d) Planted hillslopes. Note that  
455 direction of the ploughing is parallel to the slope.

### 456 3.3 Spatio-temporal patterns in sediment-associated contaminants

457 Sediment associated contaminants includes a series of chemicals that form part of a legacy of current  
458 and past natural and anthropogenic activities within the catchment. Sediment quality is highly influenced by  
459 the presence of contaminants in the water (Förstner, 1987). The Rapel river system contains high concentrations  
460 of Cu due to mining activities, as well as Mo. In addition, As is also present as a naturally-occurring contaminant  
461 associated with volcanic origins and enhanced in riverine sediment by selective transport of fine materials.  
462 Phosphorus is a typical contaminant of the area associated to the agricultural activities (Lacassie and Ruiz-Del-  
463 Solar, 2021). The spatial distribution of measured elements within the catchment (sediment in tributaries and  
464 main river courses, Fig. 4) offers evidence that enhanced Cu concentrations (Fig. 4a) have a dominant tributary

465 source that is likely influenced by mining activities that deliver sediment and leachates. These subsequently  
466 interact with sediment along the river Cachapoal from the Andes through to the Coya River, with Cu  
467 concentrations averaging  $1282 \pm 109 \text{ mg kg}^{-1}$ . Concentrations remain high in sediments near to the confluence  
468 of this tributary with the main river, values at this point “CL” (distanced around 9 km from the confluence)  
469 presented average concentrations of  $1218 \pm 87 \text{ mg kg}^{-1}$ . Moving downstream, Cu concentrations are diluted  
470 through the river Cachapoal and ultimately sediment is released into the lake with concentrations of  $453 \pm 102$   
471  $\text{mg kg}^{-1}$  (around 3 times less compared with its origin in the mine-affected tributary). Herein, sediment pulses  
472 from the tributary source (CK) to the material recovered from the lake covers a distance of 124 km along which  
473 a range of additional sediment sources are active and contributing to the mix. In comparison, Cu concentrations  
474 in the Tinguiririca river varied from values of 35 to  $118 \text{ mg kg}^{-1}$  (average  $64 \pm 14 \text{ mg kg}^{-1}$ ). These values can  
475 be considered as baseline levels in the wider basin area, as in this river there is no evidence of mining activities.  
476 Similarly, the behaviour of Mo appears to be as a secondary product of mining activities (Fig. 4b), with average  
477 concentrations in mountain reaches (CK) of  $50 \pm 3 \text{ mg kg}^{-1}$ . However, Mo concentrations in this case are not  
478 exclusively from sources derived from the Andes, as the main source of Mo into the lake comes from another  
479 mining activity located in the coastal range area in the Alhue sub-catchment (AL), where concentrations in  
480 sediments averaged  $162 \pm 74 \text{ mg kg}^{-1}$ , possibly derived from a tailing dam that accumulates mining waste for  
481 the operations taking place in the Andes. Concentrations in the lake were  $10 \pm 2 \text{ mg kg}^{-1}$ ; at least sixteen time  
482 less concentrated than the Alhue river (AL). As stated with Cu, the concentrations of Mo in the Tinguiririca  
483 River and tributaries ranged from 1 to  $8 \text{ mg kg}^{-1}$  (average  $3 \pm 1 \text{ mg kg}^{-1}$ ). These values can also be considered  
484 as background levels within the catchment.



485

486 **Fig. 4.** Spatial distribution of some sediment associated contaminants (SAC) in the Rapel Catchment. a) Cu, b)  
 487 Mo, c) P and d) As.

488 Elevated phosphorus concentrations of note appear to emanate from the dryland area (Coastal Range)  
 489 with a maximum value of  $8255 \text{ mg kg}^{-1}$  at the San Miguel stream (MI) sampling point (average value of  $5283$   
 490  $\pm 1335 \text{ mg kg}^{-1}$ ). This sampling area is located near to ‘pig farms’ and possibly highly influenced by this activity.  
 491 Concentrations from the rest of the sampling points within the catchment were similar ( $\sim 1400 \text{ mg kg}^{-1}$ ). The  
 492 concentrations detected in the lake averaged  $1443 \pm 116 \text{ mg kg}^{-1}$ . In a eutrophic lake in China P values ranged  
 493 from  $544$  to  $932 \text{ mg kg}^{-1}$  indicating the risk of P-related events in this system (Wang and Liang, 2015),  
 494 suggesting that the Rapel lake may be also be at risk of eutrophication if P is not bound stably in the sediment  
 495 column.

496 Arsenic concentrations (Fig. 4d) were higher in proximity to the Andes with average values for both  
 497 rivers of  $35 \pm 20 \text{ mg kg}^{-1}$ . Values at the lake were around  $42 \pm 2 \text{ mg kg}^{-1}$ . For the rest of the sampling points in



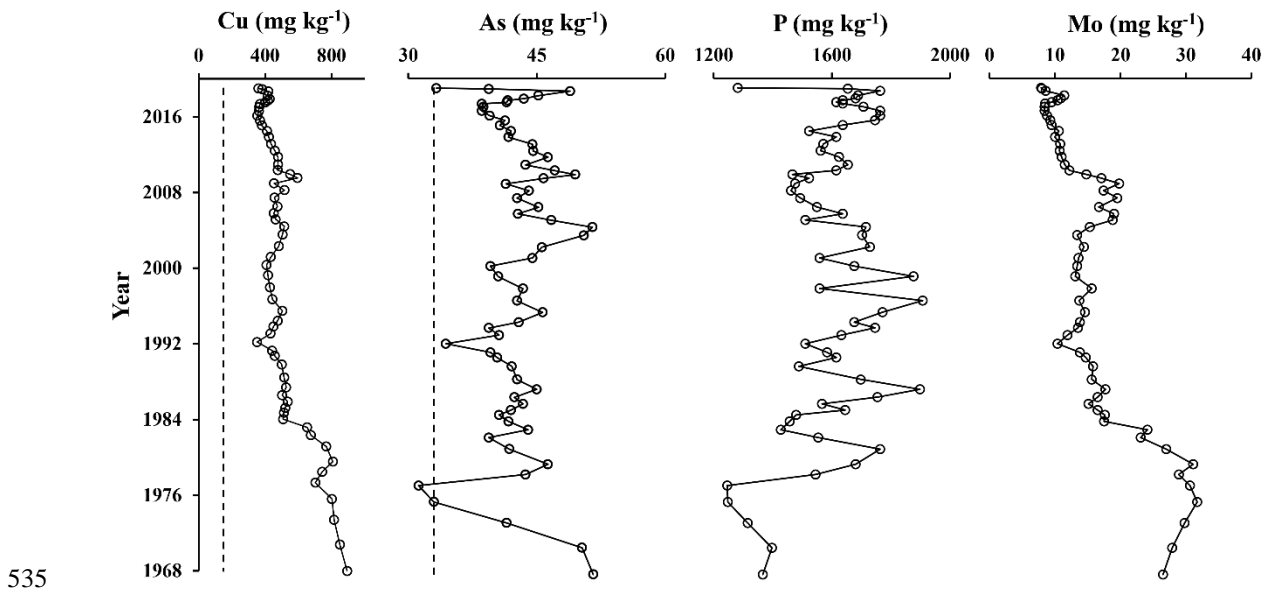
498 both rivers average values were  $24 \pm 11 \text{ mg kg}^{-1}$ . Therefore, it was concluded that the sources of As in the  
499 catchment are derived from naturally occurring As within the Andes (Lacassie and Ruiz-Del-Solar, 2021) with  
500 some enhancement by fluvial sorting (Horowitz and Elrick, 1987). Previous studies in the Rapel catchment  
501 detected maximum As concentrations of 72 and 21  $\text{mg kg}^{-1}$  in the Cachapoal and Tinguiririca Rivers  
502 respectively. Both rivers contribute sediment-associated As to the lake due to high background As  
503 concentrations in Andean geology and consequently concentrations of this element in fine sediments can reach  
504 the lake and influence its accumulation due to natural processes (Lacassie and Ruiz-Del-Solar, 2021), as well  
505 as being enhanced by mining (Figure 4d).

506 In order to establish if concentrations reported within the sediments have the potential to produce certain  
507 effect on living organisms, measured concentrations were compared to Probable Effect Concentrations (PEC)  
508 (MacDonald et al., 2000). The consensus-based PEC for elements of interest in this study are: Cu:  $149 \text{ mg kg}^{-1}$ ;  
509 As:  $33 \text{ mg kg}^{-1}$ . Regarding the Cu values, in the Tinguiririca River all concentrations in sediment samples  
510 were below the threshold suggested for this element. The other tributaries that contribute sediments directly to  
511 the lake “Las Palmas” and “Alhue” were over and below this threshold respectively. Regarding the sediment in  
512 the lake itself, concentrations were above this threshold. The samples, and as stated above, from the Cachapoal  
513 river and tributaries showed high concentrations of Cu and most of them were above the PEC. Nevertheless,  
514 samples collected at the higher part of the Andes mountains were below (CH, PA, CQ). This demonstrates the  
515 potential negative effect of Cu (present in sediments that are derived from the processing of minerals containing  
516 Cu) on aquatic living organisms in the receptor aquatic environments.

517 Concerning Arsenic values, the PEC threshold was mostly surpassed by all the sediment samples  
518 within the Cachapoal river, and only in samples collected by the Andes in the Tinguiririca River (TZ, TA, ID).  
519 Samples from sediment collected at AL and PL were below this threshold. Values of the Lake sediments also  
520 exceeded the PEC. This evidenced that natural sources of As by the mountains put in potential risk the living  
521 organisms present in this area.

522 Regarding the temporal inputs of sediment-associated contaminants into the lake, the profile for the  
523 four elements of interest (Fig. 5) and how they behaved since 1968 offer important temporal perspectives in  
524 pollution dynamics in the system. Profiles of Cu and Mo presented strong correlation ( $R: 0.92, p < 0.05$ ), this

525 is expected as those elements demonstrated to come from the same origin (mining activities). Additionally, the  
 526 mining company during the year 1985 began to use a different rock that was depleted in Cu and consequently  
 527 the amount of Cu present in the mineral was much lower than the one used before 1985. This process can be  
 528 clearly seen in the profiles for Cu and Mo with a drop in concentration in the sediment profile since 1985. Also,  
 529 the mining activity since 1985 invested in the improvements of their environmental impacts as it is clear that  
 530 Cu inputs from 1985 also tended to decrease. Nevertheless, all the values were higher than the PEC for this  
 531 element. The same is true for As concentrations where values were over the threshold and relatively constant  
 532 throughout the years. Phosphorus, on the other hand, followed a step change upward in the late 1970s, where  
 533 concentrations have remained relatively constant from 1981 potentially reflecting sustained but noting also that  
 534 the non-conservative properties of this element can also influence profiles (Tiecher et al., 2019).



536 **Fig. 5.** Profiles of concentrations of four SAC. For Cu and As segmented lines are indicative of their PEC  
 537 values.

### 538 3.4 Challenges and opportunities for sediment management in major hydropower basins

539 Adopting a holistic ‘systems-thinking’ approach is paramount in tackling hydropower sediment  
 540 management challenges that comprise the food-water-energy-environment nexus (Blake et al., 2018b).  
 541 Hydropower basins are complex systems where numerous factors, including dynamic change in land use  
 542 practice, climatic conditions and hydro-geomorphological process influence sediment dynamics. Understanding

543 these interconnected factors and their interactions, through interdisciplinary and cross-sectoral working, is  
544 crucial for devising comprehensive management plans (del Valle, 2023). Collaborative efforts between  
545 stakeholders can enhance the effectiveness of sediment management strategies and facilitate sustainable land  
546 management decisions. The Rapel River basin serves as an exemplar to demonstrate the complexity and urgency  
547 of addressing hydropower siltation where stakeholder participation and co-design will be an essential part of  
548 the solution.

549         Our analysis of sediment sources in the Rapel basin reveals that conversion of steep land from native  
550 vegetation to agriculture promotes soil erosion, making agriculture the dominant contributor of sediment to the  
551 reservoir. Mining activities also contribute to the total sediment deposited in the lake but here it is the sediment-  
552 associated contaminants such as Cu and Mo that pose significant risks to reservoir water and broader  
553 environmental quality. Industrial livestock production further intensifies the environmental quality problem,  
554 particularly through particulate P input. Our evaluation of these challenges emphasises the need for context-  
555 specific, locally tailored solutions that address the unique interplay of factors contributing to soil erosion and  
556 downstream siltation.

557         Addressing sedimentation challenges requires a collaborative participatory approach that engages  
558 stakeholders at all levels (Gerrits and Edelenbos, 2004). Stakeholder participation will play a crucial role in co-  
559 designing effective sediment management strategies. Engaging stakeholders across sectors fosters a sense of  
560 ownership of the problem and enables the integration of multiple perspectives, knowledge, and needs into  
561 decision-making processes (Armitage et al., 2010; Jager et al., 2016; Pahl-Wostl et al., 2012). Collaborative  
562 platforms, such as participatory workshops, stakeholder dialogues, and multi-stakeholder partnerships, facilitate  
563 inclusive and informed discussions, leading to more effective and socially acceptable solutions (Ayala-Orozco  
564 et al., 2018; del Valle, 2023; Reed, 2008) and empirical data such as that gathered in this study have a key role  
565 to play in eliciting discussion and supporting co-design (Blake et al., 2018b; Kelly et al., 2020).

566         In the Rapel basin, stakeholder collaboration faces potential challenges through the conflicting  
567 interests of agriculture, mining, and environmental conservation. This requires a proactive dialogue and guided  
568 negotiation to find mutually beneficial solutions. The basin comprises diverse communities and industrial sector  
569 actors with varying economic and socio-cultural contexts, necessitating equitable representation and inclusive

570 decision-making processes (del Valle, 2023). Overcoming these challenges involves building trust, fostering  
571 cooperation, and addressing power dynamics among stakeholders. Strengthening governance mechanisms and  
572 promoting institutional coordination will also be importance considerations for effective implementation of  
573 sediment management strategies in the Rapel basin. Co-designing solutions with stakeholders promotes  
574 adaptive management and iterative decision-making, allowing for the development of tailored strategies that  
575 consider the unique geomorphological, hydrological, and socio-economic characteristics of the basin (Mussehl  
576 et al., 2022).

577           The research reported in this paper was a part of a broader project in the Rapel Basin that also involved  
578 an intervention process guided by the trans-disciplinary method for conducting social transformations called  
579 Participatory Innovation Praxis (del Valle, 2023; O’Ryan and Del Valle, 1996). In this process representative  
580 actors of the basin generated a consensus understanding of the soil erosion condition and defined a  
581 comprehensive strategy to face it over the short, medium and long term. According to this understanding, soil  
582 erosion is the main symptom of a social-cultural condition existing because practically no effective action exists  
583 in any or the following social dimensions: integrated management of the basin; incentives and promotion of  
584 sustainable soil management; cultural transformation towards understanding soil as an ecosystem;  
585 dissemination of agricultural and forestry practices that activate soil’s life; mechanisms for technological  
586 innovation, development and demonstration; fostering legal instruments to promote conservation and  
587 sustainable use of soil in Chile; and sufficient and effective enforcement of norms for soil conservation and use  
588 in Chile. The strategy specifies 41 social, institutional, and technological innovations in all dimensions, along  
589 with a governance system for their participatory design and implementation.

590           Sediment management in major hydropower basins presents a global challenge exemplified by the  
591 Rapel basin (Syvitski et al., 2005). The specific challenges faced here highlight the need for sensitive co-design  
592 to produce evidence – led and context-specific solutions that address the complexity and dynamic nature of the  
593 drivers within and external to the basin and its communities. Achieving these co-designed solutions, alongside  
594 an equitable, stakeholder-led governance system for the basin is the only way to enhance the social acceptability  
595 of sediment management strategies. The research outcomes from sediment source apportionment studies have  
596 the potential to inform international best practices in sediment management for sustainable hydropower

597 development and ecosystem protection. As a representative exemplar, the Rapel Basin challenge highlights the  
598 transferability of such research findings to other hydropower basins globally, reducing the impact of soil erosion  
599 on water, food and energy security.

## 600 **4 Conclusions**

601 Evidence of spatio-temporal dynamics of sediment and pollutant source from the Rapel Basin provides  
602 an important new framework for evaluating the global hydropower siltation risk. Illuminating the complexity  
603 of basin response to land management decisions, and the complex socioeconomic and cultural factors that drive  
604 them, demonstrates the clear need for holistic, system thinking approach to derive evidence-led, co-designed  
605 solutions.

606 With the changing global climate and, in particular rainfall patterns and emerging climates of extreme,  
607 national and inter-governmental bodies are rightly focusing on adaptation and mitigation strategies to reinforce  
608 food, water and energy security through sustainable environmental management. Herein, the interplay between  
609 agriculture and mining against the background of natural sediment production in the Rapel Basin is highly  
610 relevant. Despite glacial retreat and increase in the intensity of extreme rainfall in the region, the changes in  
611 natural sediment production in the high relief Andean sub-catchments are dwarfed by agricultural and mining  
612 inputs. The coincidence of observed consequences of conversion of steep lands in the Coastal Mountain range  
613 to orchards and vineyards with changes in rainfall patterns threatens a step-change in sediment production. This  
614 non-linear response in siltation to rainfall patterns is not readily understood by stakeholders and will be seen to  
615 intensify with continued conversion of naturally-vegetated steplands. In this exemplar case, the complexity of  
616 governance issues and the combined concerns of sediment and mining pollution as well as agricultural co-  
617 contaminant further demonstrates the need for system-wide participatory solution co-design. The importance  
618 of blending scientific evidence with local environmental knowledge to inform an inclusive participatory  
619 approach to resolving basin-wide hydropower siltation problems cannot be over-emphasised as we move into  
620 new and less predictable climate regimes.

621

622 **Declaration of Competing Interest**

623           The authors declare that they have no known competing financial interests or personal relationships  
624 that could have appeared to influence the work reported in this paper.

625 **Acknowledgments**

626           This work was supported by the Joint Chile-UK Newton-Picarte Fund under UK Natural Environment  
627 Research Council (NERC) Grant NE/R015597/1 and Chilean ANID Fondecyt Project ID 1210813. The authors  
628 are also grateful for support from the International Atomic Energy Agency under ARCAL Project RLA5064  
629 and the joint UN FAO/IAEA Coordinated Research Projects (CRP) “D15017: Nuclear Techniques for a Better  
630 Understanding of the Impact of Climate Change on Soil Erosion in Upland Agro-ecosystems” and “D1.50.18:  
631 ‘Multiple Isotope Fingerprints to Identify Sources and Transport of Agro- Contaminants’”.

632

633 **5 References**

- 634 Aitken, D., Rivera, D., Godoy-Faundez, A., Holzapfel, E., 2016. Water Scarcity and the Impact of the Mining  
635 and Agricultural Sectors in Chile. *Sustainability* 8, 128. <https://doi.org/10.3390/su8020128>
- 636 Appleby, P.G., 2001. Chronostratigraphic Techniques in Recent Sediments, in: Last, W.M., Smol, J.P. (Eds.),  
637 Tracking Environmental Change Using Lake Sediments: Basin Analysis, Coring, and Chronological  
638 Techniques. Springer Netherlands, Dordrecht, pp. 171–203. [https://doi.org/10.1007/0-306-47669-X\\_9](https://doi.org/10.1007/0-306-47669-X_9)
- 639 Appleby, P.G., Oldfield, F., 1978. The calculation of lead-210 dates assuming a constant rate of supply of  
640 unsupported <sup>210</sup>Pb to the sediment. *CATENA* 5, 1–8. [https://doi.org/10.1016/S0341-8162\(78\)80002-](https://doi.org/10.1016/S0341-8162(78)80002-2)  
641 2
- 642 Armitage, D., Berkes, F., Doubleday, N., 2010. Adaptive co-management: collaboration, learning, and multi-  
643 level governance. UBC Press.
- 644 Ayala-Orozco, B., Rosell, J.A., Merçon, J., Bueno, I., Alatorre-Frenk, G., Langle-Flores, A., Lobato, A., 2018.  
645 Challenges and strategies in place-based multi-stakeholder collaboration for sustainability: Learning  
646 from experiences in the Global South. *Sustainability* 10, 3217.
- 647 Blake, W.H., Boeckx, P., Stock, B.C., Smith, H.G., Bode, S., Upadhayay, H.R., Gaspar, L., Goddard, R.,  
648 Lennard, A.T., Lizaga, I., Lobb, D.A., Owens, P.N., Petticrew, E.L., Kuzyk, Z.Z.A., Gari, B.D.,  
649 Munishi, L., Mtei, K., Nebiyu, A., Mabit, L., Navas, A., Semmens, B.X., 2018a. A deconvolutional  
650 Bayesian mixing model approach for river basin sediment source apportionment. *Sci Rep* 8, 13073.  
651 <https://doi.org/10.1038/s41598-018-30905-9>
- 652 Blake, W.H., Ficken, K.J., Taylor, P., Russell, M.A., Walling, D.E., 2012. Tracing crop-specific sediment  
653 sources in agricultural catchments. *Geomorphology* 139–140, 322–329.  
654 <https://doi.org/10.1016/j.geomorph.2011.10.036>
- 655 Blake, W.H., Kelly, C., Wynants, M., Patrick, A., Lewin, S., Lawson, J., Nasolwa, E., Page, A., Nasserri, M.,  
656 Marks, C., Gilvear, D., Mtei, K., Munishi, L., Ndakidemi, P., 2021. Integrating land-water-people  
657 connectivity concepts across disciplines for co-design of soil erosion solutions. *Land Degradation &*  
658 *Development* 32, 3415–3430. <https://doi.org/10.1002/ldr.3791>
- 659 Blake, W.H., Rabinovich, A., Wynants, M., Kelly, C., Nasserri, M., Ngondya, I., Patrick, A., Mtei, K., Munishi,  
660 L., Boeckx, P., 2018b. Soil erosion in East Africa: an interdisciplinary approach to realising pastoral  
661 land management change. *Environmental Research Letters* 13, 124014.
- 662 Blake, W.H., Wallbrink, P.J., Doerr, S.H., Shakesby, R.A., Humphreys, G.S., 2006. Magnetic enhancement in  
663 wildfire-affected soil and its potential for sediment-source ascription. *Earth Surf. Process. Landf.* 31,  
664 249–264. <https://doi.org/10.1002/esp.1247>
- 665 Bravo-Linares, C., Schuller, P., Castillo, A., Ovando-Fuentealba, L., Munoz-Arcos, E., Alarcon, O., de los  
666 Santos-Villalobos, S., Cardoso, R., Muniz, M., dos Anjos, R.M., Bustamante-Ortega, R., Dercon, G.,  
667 2018. First use of a compound-specific stable isotope (CSSI) technique to trace sediment transport in  
668 upland forest catchments of Chile. *Sci. Total Environ.* 618, 1114–1124.  
669 <https://doi.org/10.1016/j.scitotenv.2017.09.163>
- 670 Bravo-Linares, C., Schuller, P., Castillo, A., Salinas-Curinao, A., Ovando-Fuentealba, L., Muñoz-Arcos, E.,  
671 Swales, A., Gibbs, M., Dercon, G., 2020. Combining isotopic techniques to assess historical sediment  
672 delivery in a forest catchment in central Chile. *Journal of Soil Science and Plant Nutrition* 20, 83–94.  
673 <https://doi.org/10.1007/s42729-019-00103-1>
- 674 Bronstert, A., de Araújo, J.-C., Batalla, R.J., Costa, A.C., Delgado, J.M., Francke, T., Foerster, S., Guentner,  
675 A., López-Tarazón, J.A., Mamede, G.L., Medeiros, P.H., Mueller, E., Vericat, D., 2014. Process-based  
676 modelling of erosion, sediment transport and reservoir siltation in mesoscale semi-arid catchments.  
677 *Journal of Soils and Sediments* 14, 2001–2018. <https://doi.org/10.1007/s11368-014-0994-1>
- 678 Collins, A.L., Blackwell, M., Boeckx, P., Chivers, C.-A., Emelko, M., Evrard, O., Foster, I., Gellis, A.,  
679 Gholami, H., Granger, S., Harris, P., Horowitz, A.J., Laceby, J.P., Martinez-Carreras, N., Minella, J.,  
680 Mol, L., Nosrati, K., Pulley, S., Silins, U., da Silva, Y.J., Stone, M., Tiecher, T., Upadhayay, H.R.,  
681 Zhang, Y., 2020. Sediment source fingerprinting: benchmarking recent outputs, remaining challenges  
682 and emerging themes. *Journal of Soils and Sediments* 20, 4160–4193. [https://doi.org/10.1007/s11368-](https://doi.org/10.1007/s11368-020-02755-4)  
683 020-02755-4
- 684 Collins, A.L., Pulley, S., Foster, I.D.L., Gellis, A., Porto, P., Horowitz, A.J., 2017. Sediment source  
685 fingerprinting as an aid to catchment management: A review of the current state of knowledge and a  
686 methodological decision-tree for end-users. *J. Environ. Manage.* 194, 86–108.  
687 <https://doi.org/10.1016/j.jenvman.2016.09.075>

688 Davies-Colley, R.J., Smith, D.G., 2001. Turbidity, suspended sediment, and water clarity: A review. *J. Am.*  
689 *Water Resour. Assoc.* 37, 1085–1101. <https://doi.org/10.1111/j.1752-1688.2001.tb03624.x>

690 del Valle, A., 2023. Participatory Innovation Praxis: A trans-disciplinary method for conducting high-  
691 complexity social transformations. *Societal Impacts* 100004.

692 Dercon, G., Mabit, L., Hancock, G., Nguyen, M.L., Dornhofer, R., Bacchi, O.O.S., Benmansour, M., Bernard,  
693 C., Froehlich, W., Golosov, V.N., Hacıyakupoglu, S., Hai, P.S., Klik, A., Li, Y., Lobb, D.A., Onda,  
694 Y., Popa, N., Rafiq, M., Ritchie, J.C., Schuller, P., Shakhshiro, A., Wallbrink, P., Walling, D.E.,  
695 Zapata, F., Zhang, X., 2012. Fallout radionuclide-based techniques for assessing the impact of soil  
696 conservation measures on erosion control and soil quality: an overview of the main lessons learnt under  
697 an FAO/IAEA Coordinated Research Project. *J. Environ. Radioact.* 107, 78–85.  
698 <https://doi.org/10.1016/j.jenvrad.2012.01.008>

699 Fleige, H., Beck-Broichsitter, S., Dorner, J., Goebel, M.-O., Bachmann, J., Horn, R., 2016. Land use and soil  
700 development in southern Chile: Effects on physical properties. *J. Soil Sci. Plant Nutr.* 16, 818–831.

701 Förstner, U., 1987. Sediment-associated contaminants—an overview of scientific bases for developing remedial  
702 options. *Hydrobiologia* 149, 221–246.

703 Gaspar, L., Blake, W.H., Lizaga, I., Latorre, B., Navas, A., 2022. Particle size effect on geochemical  
704 composition of experimental soil mixtures relevant for unmixing modelling. *Geomorphology* 403,  
705 108178. <https://doi.org/10.1016/j.geomorph.2022.108178>

706 Gaspar, L., Lizaga, I., Blake, W.H., Latorre, B., Quijano, L., Navas, A., 2019. Fingerprinting changes in source  
707 contribution for evaluating soil response during an exceptional rainfall in Spanish pre-pyrenees.  
708 *Journal of Environmental Management* 240, 136–148. <https://doi.org/10.1016/j.jenvman.2019.03.109>

709 Gerrits, L., Edelenbos, J., 2004. Management of sediments through stakeholder involvement. *Journal of Soils*  
710 *and Sediments* 4, 239–246. <https://doi.org/10.1007/BF02991120>

711 Haddadchi, A., Ryder, D.S., Evrard, O., Olley, J., 2013. Sediment fingerprinting in fluvial systems: review of  
712 tracers, sediment sources and mixing models. *International Journal of Sediment Research* 28, 560–  
713 578. [https://doi.org/10.1016/S1001-6279\(14\)60013-5](https://doi.org/10.1016/S1001-6279(14)60013-5)

714 Horowitz, A.J., Elrick, K.A., 1987. The relation of stream sediment surface area, grain size and composition to  
715 trace element chemistry. *Applied Geochemistry* 2, 437–451. [https://doi.org/10.1016/0883-2927\(87\)90027-8](https://doi.org/10.1016/0883-2927(87)90027-8)

716

717 Jager, N.W., Challies, E., Kochskämper, E., Newig, J., Benson, D., Blackstock, K., Collins, K., Ernst, A., Evers,  
718 M., Feichtinger, J., 2016. Transforming European water governance? Participation and river basin  
719 management under the EU Water Framework Directive in 13 member states. *Water* 8, 156.

720 Kelly, C., Wynants, M., Munishi, L.K., Nasser, M., Patrick, A., Mtei, K.M., Mkilema, F., Rabinovich, A.,  
721 Gilvear, D., Wilson, G., 2020. ‘Mind the Gap’: reconnecting local actions and multi-level policies to  
722 bridge the governance gap. An example of soil erosion action from East Africa. *Land* 9, 352.

723 Kitch, J.L., Phillips, J., Peukert, S., Taylor, A., Blake, W.H., 2019. Understanding the geomorphic consequences  
724 of enhanced overland flow in mixed agricultural systems: sediment fingerprinting demonstrates the  
725 need for integrated upstream and downstream thinking. *J. Soils Sediments* 19, 3319–3331.  
726 <https://doi.org/10.1007/s11368-019-02378-4>

727 Kondolf, G.M., Gao, Y., Annandale, G.W., Morris, G.L., Jiang, E., Zhang, J., Cao, Y., Carling, P., Fu, K., Guo,  
728 Q., 2014. Sustainable sediment management in reservoirs and regulated rivers: Experiences from five  
729 continents. *Earth’s Future* 2, 256–280.

730 Lacassie, J.P., Ruiz-Del-Solar, J., 2021. Integrated mineralogical and geochemical study of the Rapel fluvial  
731 system, central Chile: An application of multidimensional analysis to river sedimentation. *Journal of*  
732 *South American Earth Sciences* 109, 103289. <https://doi.org/10.1016/j.jsames.2021.103289>

733 Laceyby, J.P., Evrard, O., Smith, H.G., Blake, W.H., Olley, J.M., Minella, J.P.G., Owens, P.N., 2017. The  
734 challenges and opportunities of addressing particle size effects in sediment source fingerprinting: A  
735 review. *Earth-Sci. Rev.* 169, 85–103. <https://doi.org/10.1016/j.earscirev.2017.04.009>

736 Lecaros Sánchez, M.H., 2011. Estudio de sedimentación en el embalse Rapel (Undergraduate dissertation).  
737 Universidad de Chile, <https://repositorio.uchile.cl/handle/2250/104338>.

738 Li, Z., Fang, H., 2016. Impacts of climate change on water erosion: A review. *Earth-Science Reviews* 163, 94–  
739 117. <https://doi.org/10.1016/j.earscirev.2016.10.004>

740 MacDonald, D.D., Ingersoll, C.G., Berger, T.A., 2000. Development and evaluation of consensus-based  
741 sediment quality guidelines for freshwater ecosystems. *Archives of environmental contamination and*  
742 *toxicology* 39, 20–31.



743 Martinez-Carreras, N., Krein, A., Udelhoven, T., Gallart, F., Iffly, J.F., Hoffmann, L., Pfister, L., Walling, D.E.,  
744 2010. A rapid spectral-reflectance-based fingerprinting approach for documenting suspended sediment  
745 sources during storm runoff events. *J. Soils Sediments* 10, 400–413. [https://doi.org/10.1007/s11368-](https://doi.org/10.1007/s11368-009-0162-1)  
746 009-0162-1

747 Muñoz-Arcos, E., Castillo, A., Cuevas-Aedo, A., Ovando-Fuentealba, L., Taylor, A., Bustamante-Ortega, R.,  
748 Blake, W.H., Bravo-Linares, C., 2021. Sediment source apportionment following wildfire in an upland  
749 commercial forest catchment. *Journal of Soils and Sediments* 21, 2432–2449.  
750 <https://doi.org/10.1007/s11368-021-02943-w>

751 Mussehl, M.L., Horne, A.C., Webb, J.A., Poff, N.L., 2022. Purposeful stakeholder engagement for improved  
752 environmental flow outcomes. *Frontiers in Environmental Science* 9, 749864.

753 O’Ryan, R., Del Valle, A., 1996. Managing air quality in Santiago: what needs to be done? *Estudios de*  
754 *Economía* 23, 155–191.

755 Owens, P.N., 2020. Soil erosion and sediment dynamics in the Anthropocene: a review of human impacts during  
756 a period of rapid global environmental change. *J. Soils Sediments* 20, 4115–4143.  
757 <https://doi.org/10.1007/s11368-020-02815-9>

758 Owens, P.N., Blake, W.H., Gaspar, L., Gateuille, D., Koiter, A.J., Lobb, D.A., Petticrew, E.L., Reiffarth, D.G.,  
759 Smith, H.G., Woodward, J.C., 2016. Fingerprinting and tracing the sources of soils and sediments:  
760 Earth and ocean science, geoarchaeological, forensic, and human health applications. *Earth-Sci. Rev.*  
761 162, 1–23. <https://doi.org/10.1016/j.earscirev.2016.08.012>

762 Pahl-Wostl, C., Lebel, L., Knieper, C., Nikitina, E., 2012. From applying panaceas to mastering complexity:  
763 toward adaptive water governance in river basins. *Environmental Science & Policy* 23, 24–34.

764 Pepin, E., Carretier, S., Guyot, J.-L., Escobar, F., 2010. Specific suspended sediment yields of the Andean rivers  
765 of Chile and their relationship to climate, slope and vegetation. *Hydrological Sciences Journal—Journal*  
766 *des Sciences Hydrologiques* 55, 1190–1205.

767 Perera, D., Williams, S., Smakhtin, V., 2023. Present and future losses of storage in large reservoirs due to  
768 sedimentation: a country-wise global assessment. *Sustainability* 15, 219.

769 Pizarro, J., Rubio, M.A., Castillo, X., 2003. Study of chemical speciation in sediments: An approach to vertical  
770 metals distribution in Rapel reservoir (Chile). *Journal of the Chilean Chemical Society* 48, 45–50.

771 Poesen, J., 2018. Soil erosion in the Anthropocene: Research needs. *Earth Surface Processes and Landforms*  
772 43, 64–84. <https://doi.org/10.1002/esp.4250>

773 Reed, M.S., 2008. Stakeholder participation for environmental management: a literature review. *Biological*  
774 *conservation* 141, 2417–2431.

775 Rodgers, K., McLellan, I., Peshkur, T., Williams, R., Tonner, R., Knapp, C.W., Henriquez, F.L., Hursthouse,  
776 A.S., 2020. The legacy of industrial pollution in estuarine sediments: spatial and temporal variability  
777 implications for ecosystem stress. *Environmental Geochemistry & Health* 42, 1057–1068.

778 Rossel, V., de la Fuente, A., 2015. Assessing the link between environmental flow, hydropeaking operation and  
779 water quality of reservoirs. *Ecological Engineering* 85, 26–38.

780 Schuller, P., Walling, D.E., Iroume, A., Quilodran, C., Castillo, A., Navas, A., 2013. Using Cs-137 and Pb-  
781 210(ex) and other sediment source fingerprints to document suspended sediment sources in small  
782 forested catchments in south-central Chile. *J. Environ. Radioact.* 124, 147–159.  
783 <https://doi.org/10.1016/j.jenvrad.2013.05.002>

784 Schulz, J.J., Cayuela, L., Echeverria, C., Salas, J., Rey Benayas, J.M., 2010. Monitoring land cover change of  
785 the dryland forest landscape of Central Chile (1975–2008). *Applied Geography* 30, 436–447.  
786 <https://doi.org/10.1016/j.apgeog.2009.12.003>

787 Smith, H.G., Blake, W.H., 2014. Sediment fingerprinting in agricultural catchments: A critical re-examination  
788 of source discrimination and data corrections. *Geomorphology* 204, 177–191.  
789 <https://doi.org/10.1016/j.geomorph.2013.08.003>

790 Smith, H.G., Karam, D.S., Lennard, A.T., 2018. Evaluating tracer selection for catchment sediment  
791 fingerprinting. *Journal of Soils and Sediments* 18, 3005–3019. [https://doi.org/10.1007/s11368-018-](https://doi.org/10.1007/s11368-018-1990-7)  
792 1990-7

793 Stenberg, L., Finer, L., Nieminen, M., Sarkkola, S., Koivusalo, H., 2015. Quantification of ditch bank erosion  
794 in a drained forested catchment. *Boreal Environ. Res.* 20, 1–18.

795 Stock, B.C., Jackson, A.L., Ward, E.J., Parnell, A.C., Phillips, D.L., Semmens, B.X., 2018. Analyzing mixing  
796 systems using a new generation of Bayesian tracer mixing models. *PeerJ* 6, e5096.  
797 <https://doi.org/10.7717/peerj.5096>

798 Syvitski, J.P., Vörösmarty, C.J., Kettner, A.J., Green, P., 2005. Impact of humans on the flux of terrestrial  
799 sediment to the global coastal ocean. *science* 308, 376–380.

800 Thrush, S.F., Hewitt, J.E., Cummings, V., Ellis, J.I., Hatton, C., Lohrer, A., Norkko, A., 2004. Muddy waters:  
801 elevating sediment input to coastal and estuarine habitats. *Front. Ecol. Environ.* 2, 299–306.  
802 <https://doi.org/10.2307/3868405>

803 Tiecher, T., Ramon, R., Laceby, J.P., Evrard, O., Minella, J.P.G., 2019. Potential of phosphorus fractions to  
804 trace sediment sources in a rural catchment of Southern Brazil: Comparison with the conventional  
805 approach based on elemental geochemistry. *Geoderma* 337, 1067–1076.  
806 <https://doi.org/10.1016/j.geoderma.2018.11.011>

807 UNCCD, World Bank, 2016. Land for life. Create Wealth, Transform lives.

808 Upadhayay, H.R., Bodé, S., Griepentrog, M., Bajracharya, R.M., Blake, W., Cornelis, W., Boeckx, P., 2018.  
809 Isotope mixing models require individual isotopic tracer content for correct quantification of sediment  
810 source contributions. *Hydrological Processes* 32, 981–989. <https://doi.org/10.1002/hyp.11467>

811 Vila, I., Contreras, M., Montecino, V., Pizarro, J., Adams, D.D., 2000. Rapel: A 30 years temperate reservoir.  
812 Eutrophication or contamination? *Ergebnisse der Limnologie* 55, 31–44.

813 Walling, D.E., 2013. The evolution of sediment source fingerprinting investigations in fluvial systems. *J. Soils  
814 Sediments* 13, 1658–1675. <https://doi.org/10.1007/s11368-013-0767-2>

815 Wang, L., Liang, T., 2015. Distribution characteristics of phosphorus in the sediments and overlying water of  
816 Poyang lake. *PLoS One* 10, e0125859. <https://doi.org/10.1371/journal.pone.0125859>

817 Wharton, G., Mohajeri, S.H., Righetti, M., 2017. The pernicious problem of streambed colmation: a multi-  
818 disciplinary reflection on the mechanisms, causes, impacts, and management challenges: The  
819 pernicious problem of streambed colmation. *Wiley interdisciplinary reviews. Water* 4, e1231.  
820 <https://doi.org/10.1002/wat2.1231>

821 Wohl, E., 2015. Legacy effects on sediments in river corridors. *Earth-science reviews* 147, 30–53.  
822 <https://doi.org/10.1016/j.earscirev.2015.05.001>

823 Wynants, M., Millward, G., Patrick, A., Taylor, A., Munishi, L., Mtei, K., Brendonck, L., Gilvear, D., Boeckx,  
824 P., Ndakidemi, P., Blake, W.H., 2020. Determining tributary sources of increased sedimentation in  
825 East-African Rift Lakes. *Science of The Total Environment* 717, 137266.  
826 <https://doi.org/10.1016/j.scitotenv.2020.137266>

827 Zhang, X., Li, H.-Y., Deng, Z.D., Ringler, C., Gao, Y., Hejazi, M.I., Leung, L.R., 2018. Impacts of climate  
828 change, policy and Water-Energy-Food nexus on hydropower development. *Renewable Energy* 116,  
829 827–834. <https://doi.org/10.1016/j.renene.2017.10.030>

830